Published by IOP Publishing for Sissa Medialab

Received: *December 11, 2019*
Accepted: *January 16, 2020*
Published: *February 20, 2020*

International Workshop on Fast Cherenkov Detectors
Photon detection, DIRC design and DAQ
September 11–13, 2019, Giessen, Germany

DIRC options for the Super Charm Tau Factory

M. Schmidt,[a,1] **M. Düren,**[a] **A. Hayrapetyan,**[a] **A.Yu. Barnyakov**[b] **and S.A. Kononov**[b]

[a] *II. Physikalisches Institut, Justus Liebig University of Giessen, Giessen, Germany*
[b] *Budker Institute of Nuclear Physics, Novosibirsk, Russia*

E-mail: mustafa.a.schmidt@exp2.physik.uni-giessen.de

Abstract: The Super Charm Tau Factory (SCTF) is a future facility to be built in Novosibirsk (Russia). It mainly addresses unanswered questions regarding the Standard Model (SM) of particle physics such as flavor violating decays and charmonium states beyond the open-charm threshold. SCTF is going to provide a luminosity up to $10^{35}\,\mathrm{cm}^{-2}\mathrm{s}^{-1}$ with a center of mass (CMS) energy between 2 and 6 GeV. The physics programs studied in SCTF require excellent particle identification of muons and charged pions especially in the low momentum regime. In particular, the accurate separation of both particle species at momenta between 0.2 and 1.5 GeV is very important. Two Cherenkov detectors, based on the principle of detection of internally reflected Cherenkov radiation (DIRC), are proposed to cover the desired phase space over the full solid angle. Both detectors, the Endcap Disc DIRC (EDD) and the Barrel DIRC, have been originally designed for pion/kaon separation in the future PANDA detector at FAIR in Germany and need to be adapted and optimized for the SCTF detector in order to achieve the desired Cherenkov angle resolution of less than 1 mrad for particle momenta around 1 GeV/c.

Keywords: Cherenkov detectors; Particle identification methods

[1]Corresponding author.

https://doi.org/10.1088/1748-0221/15/02/C02032

Contents

2020 JINST 15 C02032

1 Introduction

The Super Charm Tau Factory (SCTF) is a future electron-positron collider in Novosibirsk (Russia) that is designed to answer many open questions in the field of lepton flavor violation and charmonium physics [1]. The main goal is to find new physics in so-far unobserved lepton decays like $\tau \longrightarrow \mu + \gamma$ and to study rare decays of D mesons. In addition to that, the possibility of a longitudinal beam polarization over the full energy range improves searches especially for possible CP violations in particle decays [2]. For all these physics programs, a high luminosity of up to $10^{35}\,\mathrm{cm}^{-2}\mathrm{s}^{-1}$ is required in order to obtain statistics that is by at least 2 orders of magnitude higher than in other lepton-lepton colliders such as Belle-II or BESIII. The center of mass (CMS) energy can be varied between 2 and 6 GeV depending on the investigated physics program in order to reduce and investigate background processes.

A 3D drawing of the SCTF detector is shown on the left side of figure 1. Due to equal beam energies, the detector design will be fully symmetric. It is further designed as a typical onion-shell like detector around the interaction point. The innermost subdetector systems are the inner and the main tracker that are used to determine the kinematics of the charged particles by measuring the curvature of their helix tracks inside a solenoidal magnetic field of 1 T. For the tracking system, a silicon-based vertex detector and a Time Projection Chamber (TPC) have been proposed.

The surrounding shell will be occupied by particle identification (PID) detectors. Different possible systems with aerogel Cherenkov detectors for PID purposes have been already studied [3]. Another promising alternative involves two Cherenkov counters, made of fused silica, that are placed at the two endcaps, in approximately 1.1 m away from the interaction point, and a barrel

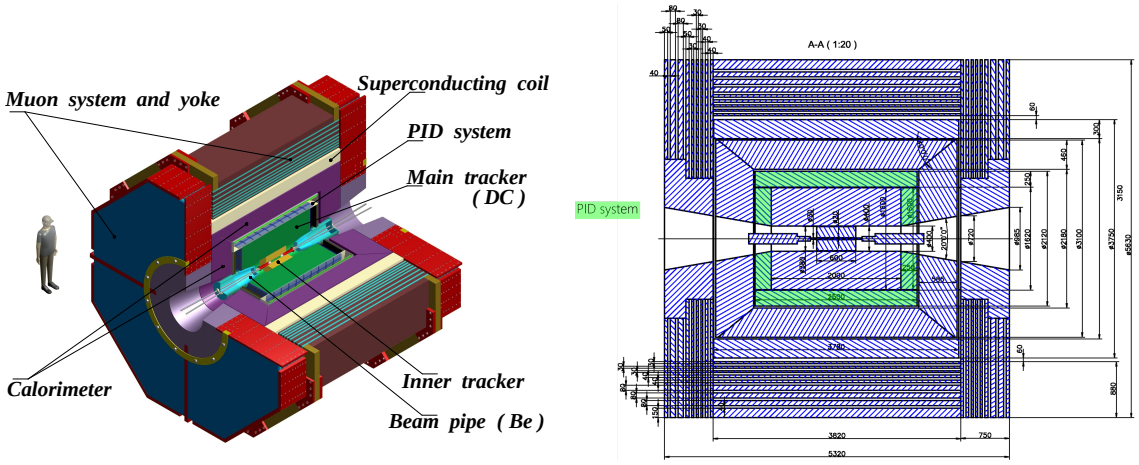

Figure 1. A 3D drawing of the future SCTF detector (left) and a sketch of the detector layout with dimensioning (right). The initially proposed area for possible PID detectors is highlighted in green.

shape detector around the interaction point with a radius between 80 and 105 cm. The proposed area is highlighted in the sketch that is shown on the right side of figure 1. However, it has to be taken into account that the detector layout is not finalized and might be changed in future. One of the most important requirements of the PID system in SCTF is the distinction of low energetic muons and charged pions in the momentum range between 0.2 and 1.5 GeV/c with a separation power of 3 standard deviations (s.d.) in order to study the rare D-meson decays and semi-leptonic D-meson decays. Around the PID subdetector system, inside the iron yoke of the solenoid magnet, muon chambers will be installed in order to detect the high energetic muons that are created during the particle interactions and secondary decays.

2 DIRC detector options

The two proposed Cherenkov detectors, based on the detection of internally reflected Cherenkov light (DIRC), are visualized in figure 2. Both designs are based on developments for the PANDA detector at FAIR in Darmstadt, Germany. A detector, similar to the PANDA Endcap Disc DIRC (EDD) [4], can be positioned at both endcaps of the SCTF detector. In order to cover the full solid angle, a Barrel-DIRC-like [5] detector for the geometrical reconstruction and/or using time of propagation (ToP) [6] information is also under consideration. This paper will focus on the optimization process of the EDD.

The actual EDD concept consists of 4 synthetic fused silica radiator plates with 98 readout modules (ROMs) on the outer rim and a radius of around 1 m, as shown in the left tile of figure 3. Each ROM consists of 3 focusing elements (FELs), containing one fused silica bar, that is going to be glued to the radiator, and a cylindrical mirror on its backside which is used to focus the Cherenkov light to the photocathode of a Microchannel Plate Photomultiplier Tube (MCP-PMT). The width of each FEL is 16 mm. The sketch of one FEL is presented in the central image of figure 3. All MCP-PMTs have the same anode structure with 3 columns and 100 pixels rows in order to provide a high single photon resolution. The size of the active area of each sensor is $50\times50\,\mathrm{mm}^2$ which results in a pixel size of around $0.5\times16\,\mathrm{mm}^2$. The right side of figure 3 illustrates the structure of the used

2020 JINST 15 C02032

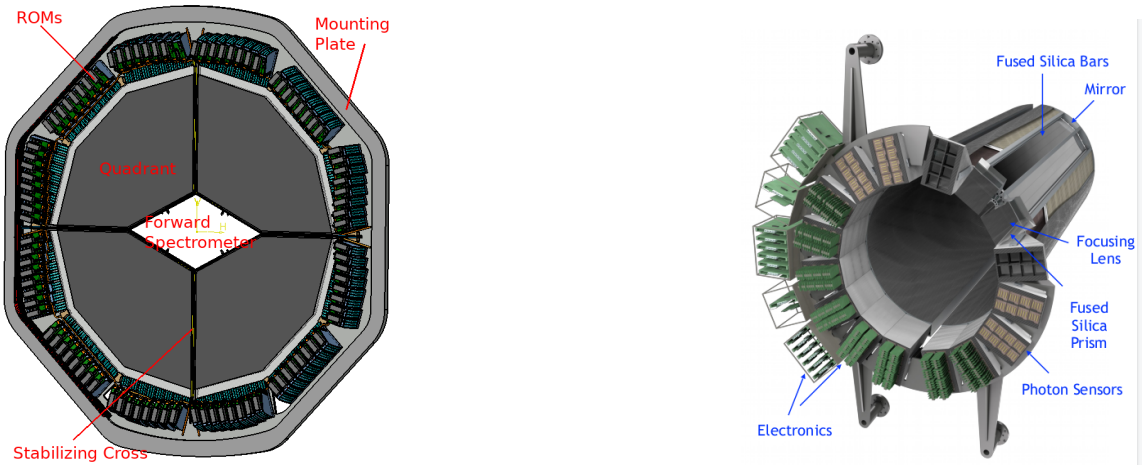

Figure 2. The design of the Endcap Disc DIRC (left) and Barrel DIRC (right). Labels indicate the most important details for the PANDA detector at FAIR. A similar design is proposed for SCTF.

MCP-PMTs together with the entry window and the segmented anode. The ASIC readout board for acquiring the photon signals is going to be attached directly to the backplane of the photon sensor.

The PANDA Barrel DIRC detector contains 16 expansion volumes with 3 fused silica bars attached to each of them. An additional lens between the bars and the expansion volumes are used to focus the Cherenkov light, whereas the focal plan is identical to the photocathode of the attached MCP-PMTs. 8 of these MCP-PMTs are attached to one expansion volume in the arrangement of a 2×4 matrix. The anode of each MCP-PMT is structured in a 8×8 pixel matrix which is sufficient to provide the required Cherenkov angle resolution. The sensor sizes are equal to the ones that are proposed for the EDD. Thus, the pixel size is given as $6.25 \times 6.25\,\mathrm{mm}^2$.

3 DIRC detector requirements

The required resolution σ of any detector can theoretically be calculated by the difference of the mean values μ_i of the determined parameter divided by the desired separation power n_σ:

$$\sigma = \frac{|\mu_2 - \mu_1|}{n_\sigma} \,. \tag{3.1}$$

The Time of Flight (ToF) of a particle is given by the fraction of the distance s between two measurement points and its speed $v = \beta c$. The β value can be written as a function of the particle momentum:

$$\beta = \frac{p}{E} = \frac{p}{\sqrt{p^2 + m^2}} \,. \tag{3.2}$$

This leads to the following formula for the computation of the ToF resolution for separating 2 particle species with the rest masses m_1 and m_2:

$$\sigma_t = \frac{s}{c n_\sigma} \left(\frac{s\sqrt{p^2 + m_2^2}}{p} - \frac{s\sqrt{p^2 + m_1^2}}{p} \right) \tag{3.3}$$

2020 JINST 15 C02032

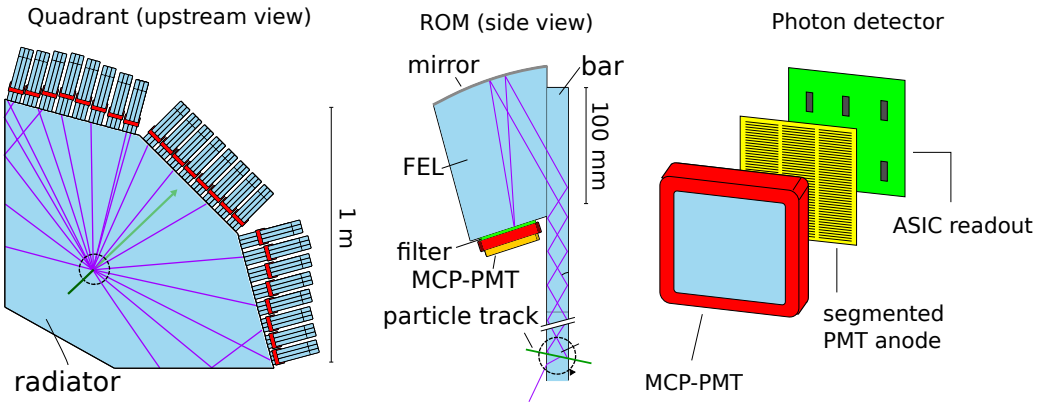

Figure 3. The schematics of the Endcap Disc DIRC for PANDA at FAIR [7].

Figure 4 shows the calculated theoretical resolutions as a function of particle momentum for a ToF system with a distance $s = 1$ m to the particle vertex. The time resolution of around 2 ps, required for a separation of 3 s.d. at 1.5 GeV/c, is not easily achievable, and the main limiting factor is the intrinsic time resolution of the detector system.

For a Cherenkov detector, the angular resolution refers to the theoretical Cherenkov angles that can be calculated according to

$$\theta_c = \arccos\left(\frac{1}{n\beta}\right) \tag{3.4}$$

where n is the refractive index of the radiator material. Replacing β again with eq. (3.2) leads to the following formula to calculate the Cherenkov angle resolution of any DIRC detector:

$$\sigma_{\theta_c} = \frac{1}{n_\sigma}\left(\arccos\left(\frac{\sqrt{p^2 + m_2^2}}{np}\right) - \arccos\left(\frac{\sqrt{p^2 + m_1^2}}{np}\right)\right) \tag{3.5}$$

The plot on the bottom of figure 4 indicates the overall detector resolution σ_{det} as a function of the particle momentum. For a 3 s.d. separation of pions and kaons at 4 GeV/c, like e.g. in the PANDA detector, a resolution of 2.1 mrad is needed. A separation of pions and muons at 1.5 GeV/c momentum with a similar separation power requires a 3 times better resolution of around 0.6 mrad. A separation for lower momenta, like e.g. 1 GeV/c, can be achieved more easy since a resolution of approximately 1.5 mrad is in principle sufficient.

In general, the detector resolution σ_{tot} of a Cherenkov counter can be split into two components: a systematic error σ_{sys} and a stochastic part σ_{stoch} to be combined quadratically:

$$\sigma_{\text{tot}}^2 = \sigma_{\text{sys}}^2 + \frac{\sigma_{\text{stoch}}^2}{N} \tag{3.6}$$

The stochastic part includes all errors related to the photon trajectory inside the Cherenkov detector, such as chromatic dispersion and intrinsic geometrical detector resolutions. This error scales with the square root of the number N of detected photons of each track. The systematic error is a fixed value for every track and includes external errors of the tracking detectors and angle straggling of the charged particle inside the radiator material.

2020 JINST 15 C02032

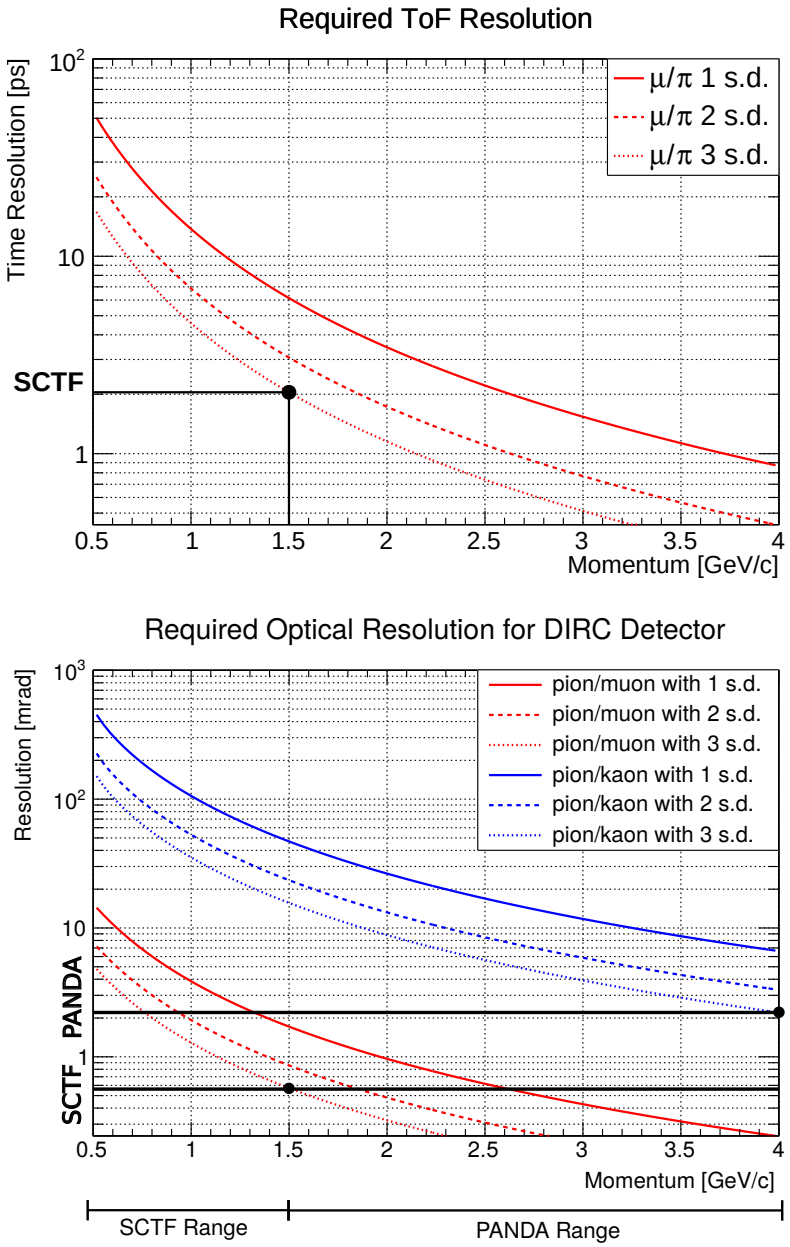

Figure 4. The required ToF (top) and Cherenkov angle resolution (bottom) for different detector systems that can be used for particle identification.

The refractive index is a function of the photon wavelength. The corresponding dispersion error is usually a limiting factor in an endcap DIRC detector since it smears time and space information of the Cherenkov angle. The left side of figure 5 illustrates the dispersion effect for 4 different particle species. In principle, there are two straight-forward possibilities to reduce the overlap between the bands: higher photon statistics, and a dedicated wavelength cut, depending on the quantum efficiency (QE) of the attached MCP-PMT. A third possibility, that includes the dispersion correction by using the time information, will be discussed later.

2020 JINST 15 C02032

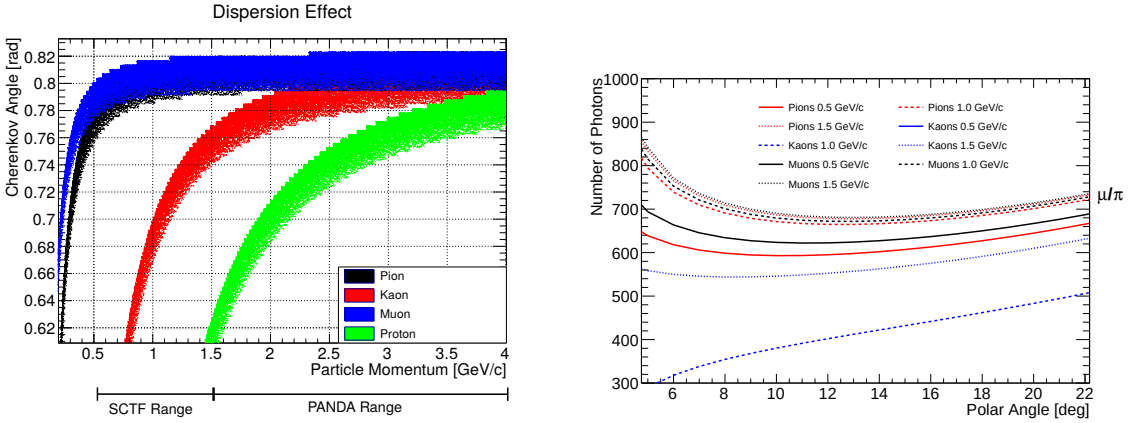

Figure 5. The influence of dispersion on the Cherenkov angle (left) and the number of photons that are trapped inside a DIRC detector as a function of momentum and polar angle (right).

In a DIRC detector, most of the photons are trapped inside the radiator material due to their internal reflection on the polished radiator surfaces. The fraction of trapped and lost photons depends mainly on the particle momentum and on the polar angle. The theoretical calculations of the trapping coefficient for muons, pions, and kaons at different momenta are presented in figure 5 (right panel). The largest amount of trapped photons can be obtained for higher momenta ($\beta \longrightarrow 1$), which influences the detector resolution positively by obtaining a higher photon yield in this critical part of the phase space.

4 PANDA EDD detector performance

The plot on the left side of figure 6 shows the likelihood difference distributions of the current EDD design for PANDA for pions and muons. The separation power can easily be calculated from eq. (3.1) by taking the average value of both standard deviations into account:

$$n_\sigma = \frac{|\mu_2 - \mu_1|}{\frac{1}{2}(\sigma_1 + \sigma_2)} \tag{4.1}$$

This determination of the separation power has been determined for a polar angle of 12° and a momentum of 1 GeV/c for μ^+ and π^+ particles. The simulation results have shown that the actual EDD design for PANDA delivers a separation power of approximately 1.5 s.d. for the chosen parameters.

In order to validate the results for different particle momenta, a momentum scan has been performed within the same Monte-Carlo (MC) framework. The results are presented on the right side of figure 6. As expected, the separation power is sufficiently high for low momentum particles around 0.5 GeV/c. However, for high momenta around 1.5 GeV/c it drops to values around 1 s.d. because of the deteriorated Cherenkov angle resolution. We aim to improve the detector resolution to a value of better than 1 mrad for particle momenta around 1.5 GeV/c.

2020 JINST 15 C02032

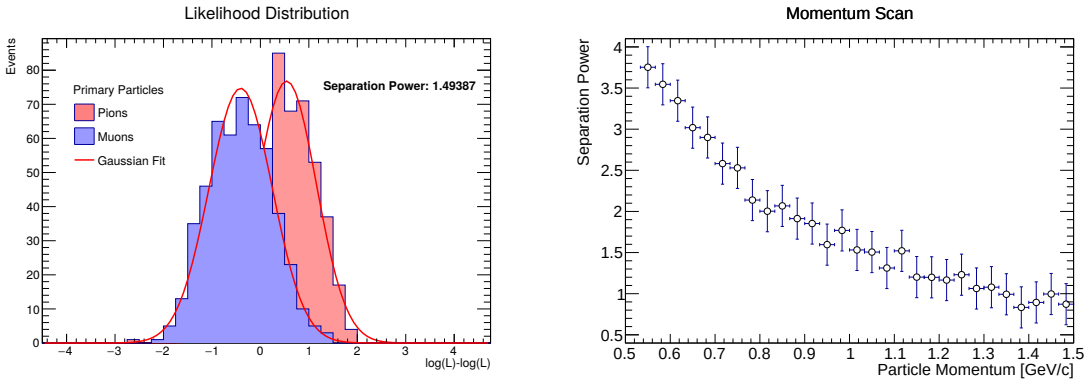

Figure 6. The obtained separation power at a momentum of 1 GeV/c and a polar angle of 12° from the likelihood differences (left) and a momentum scan for the obtainable separation power for the same polar angle (right).

5 Optimization simulations

For achieving the required resolution of 0.7 mrad for 1.5 GeV/c muon/pion separation, different upgrade scenarios have been studied. The most important optimization parameters together with the desired effects are summarized as follows:

1. Radiator thickness: varying the thickness of the radiator plate can increase the photon yield and reduce the stochastic errors.

2. Bar width: decreasing the bar width might improve the angular resolution if the number of detected photons remains nearly constant.

3. Pixel pitch: reducing the pixel pitch and increasing the number of pixels in the photon detectors can also increase the detector performance in case of proper focusing.

In addition to the above mentioned points, a better resolution can also be achieved with more radical solutions like choosing different sensor/readout combinations or developing a new focusing optics with an enhanced optical resolution.

For optimization purposes, the geometries of both described DIRC detectors have been implemented in a Geant4 framework including all relevant optical and mechanical parameters, such as the efficiencies of the proposed MCP-PMTs, the transmission losses in the radiator material, and the reflectivity of the mirror on the backside of the attached FELs. The reconstruction has been performed using a dedicated algorithm that has already been described in a previous publication [8].

5.1 Radiator thickness

In figure 7a, the number of photon hits per track is plotted as a function of the radiator thickness. Linear dependency is expected according to theoretical calculations based on the Frank-Tamm equation. The results show that energy loss and pixel occupancy do not have any significant influence on the photon detection in that detection range.

Interestingly, the plot in figure 7b indicates a maximum achievable resolution for a radiator thickness around 7 mm. For thinner radiator plates, the performance degrades due to a lower photon

2020 JINST 15 C02032

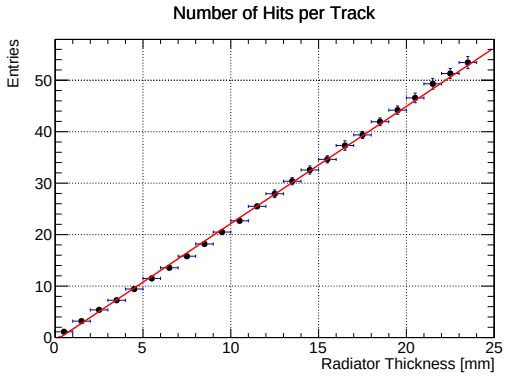

(a) Linear dependency of the number of detected photons as a function of the radiator thickness.

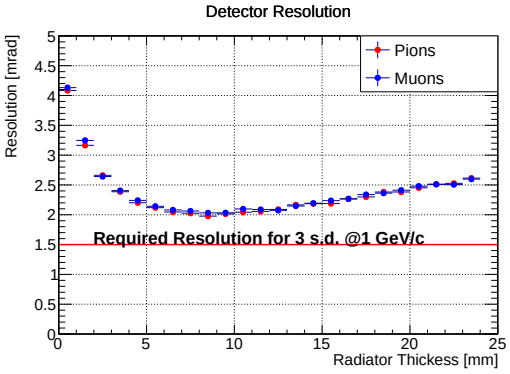

(b) Simulated detector resolution with respect to the radiator thickness compared to the required resolution.

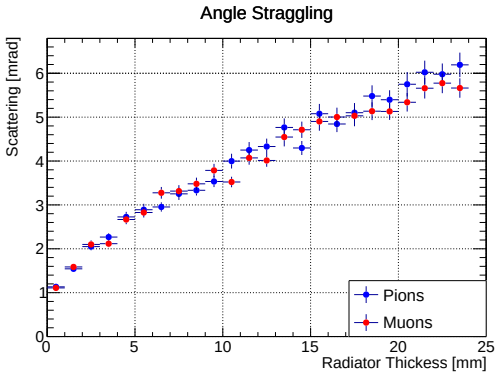

(c) Correlation between the angle straggling of pions and muons as a result of multiple Coloumb scattering and radiator thickness.

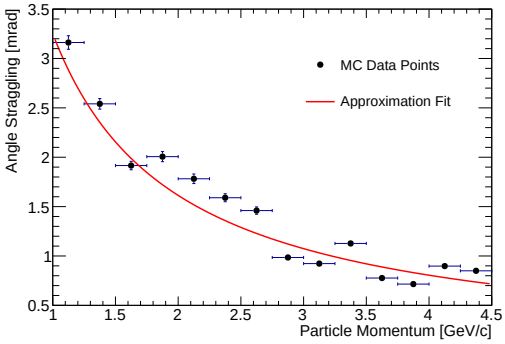

(d) Dependency of angle straggling on particle momentum for simulated pion tracks.

Figure 7. Influence of radiator thickness on the detector performance resulting from increasing photon yield and angle straggling taken from Monte-Carlo studies.

yield. For radiators with a larger thickness, an almost linear dependency between the resolution and radiator thickness can be observed.

This effect is mainly caused by the angular straggling of the charged particle due to multiple Coulomb scattering in the radiator material as shown in the plot of figure 7c. This graph illustrates the dependency of the RMS value of the angular difference between the outgoing and entering particle trajectory close to the radiator surfaces. The systematic error that influences the detector resolution scales with a factor of $\sqrt{3} \approx 1.73$. Thus, the influence of the straggling effect around 7 mm thickness can be estimated to 1.8 mrad, which is in the order of the overall detector resolution. Therefore, it can be concluded that the left part of the resolution plot is dominated by statistics and scales with $\sqrt{N}$, whereas the influence of angle straggling dominates within the right part.

The plot in figure 7d shows the dependency of the angle straggling on the particle momentum for a radiator with a thickness of 10 mm with a fit through the data points according to the related equation that describes angle straggling of charged particles in matter [9]. At momenta around 4 GeV/c, which matches with the PID settings in PANDA, the effect of angle straggling on the

2020 JINST 15 C02032

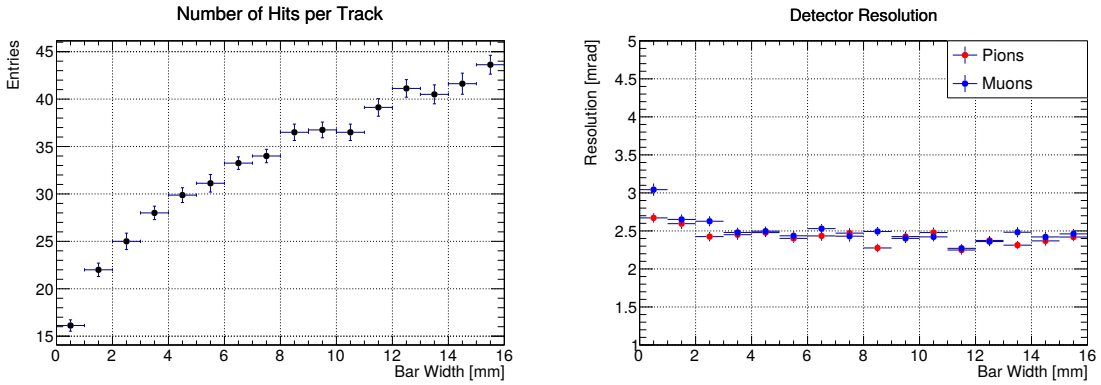

Figure 8. The number of detected photons (left) and Cherenkov angle resolution (right) as a function of the bar width.

detector resolution can be neglected. In order to reduce this effect even for lower particle momenta, the installation of additional tracking stations behind the radiator plate with a spatial resolution of around 100 μm is currently under consideration. Possible detectors could be silicon detectors with a high pixel granularity or Gas Electron Multiplier (GEM) detectors.

5.2 Bar width

Another possibility to increase detector resolution is to shrink the bar width of the FELs from the actual value of 16 mm to much smaller values. This reduces the geometrical error especially for larger polar angles, because the entering points of each photon can be determined more precisely. However, the distances between each FEL has to remains nearly constant in order to stabilize them mechanically and to avoid tunneling photons from one FEL to the other.

This condition decreases the number of detected hits for smaller bars width drastically, because the effective area seen as the ratio of bar width to the bar distance decreases for smaller bar widths. Hence, the photon yield is reduced from around 40 to 45 hits per event at a bar width of 16 mm to approximately 20 to 25 hits for bar widths at 2 mm. This dependency is shown on the left side of figure 8.

It can be already predicted that a possible increase of the single photon resolution will be deteriorated due to insufficient statistics. Indeed, this behavior is confirmed by MC studies and is presented on the right side of figure 8. As shown in this plot, the overall detector resolution remains almost unchanged for a wide interval of bar width and even gets worse for thinner bars.

5.3 Pixel size

The actual design guarantees a sufficient resolution of around 2 mrad for pion/kaon separation even up to a momentum of 4 GeV/c. Because of the quantization of the number of reflections in the bars, there are discontinuities, which can cause one more reflection of the photons inside the bars, leading to different reflection points on the mirror. In addition to that, for production reasons, the mirror has a cylindrical instead of a parabolic shape, which prevents perfect photon focusing. The spot in the focal plane has a broader extent because of additional reflection and geometrical aberration of the cylindrical mirror. The resulting spot width, that also depends on the angle of incidence, has been

2020 JINST 15 C02032

measured for different samples and is shown in the top panels of figure 9: it varies between 0.3 mm and 0.7 mm for certain angles.

The current development of the EDD uses photodetector pixel sizes of 0.5 mm. Due to the large spot width it is therefore expected, that an increase of the number of pixels in one row does not increase the detector performance sufficiently. The results of dedicated MC studies are shown at the bottom of figure 9. A slight increase of the resolution can be observed for very small pixel pitches, but the large error bars do not allow for a quantitative comparison between the different widths. Therefore, it is impossible to increase the detector resolution by changing the pixel size without optimizing the focusing optics.

5.4 Optics & sensors

The width of the projected spot is related to cylindrical/spherical mirror geometry. However, in the case of EDD this effect can be minimized by choosing a symmetrical *mushroom*-like FEL design. By attaching SiPMs instead of MCP-PMTs, substantial shrinkage of photon sensor size is possible. This leads to a higher time resolution σ_t which can be used to minimize the dispersion effects in fused silica and to increase the separation power by increasing the overall Cherenkov angle resolution. This method is called 3D-DIRC-principle and had already been considered in one of the earlier development stages of the PANDA EDD. There, 3D-DIRC got rejected because of insufficient radiation hardness of the available SiPMs [10]. Since a smaller hadronic background is expected in SCTF compared to PANDA, this option might become interesting again. However, it has to be taken into account that the intrinsic time resolution of SiPMs is far worse than the one of MCP-PMTs which counteracts the desired effect.

With a new development of SiPMs at CERN, interesting results regarding time and spatial resolution were obtained [11]. These detectors have an active area of $11 \times 15\,\mathrm{mm}^2$ and are subdivided into 16 independent strips. This leads to a pixel width of around 0.68 mm which is larger than the pixel pitch of the currently used MCP-PMTs. However, an optimization process is still ongoing and the number of strips might be enlarged. Furthermore, a good time resolution of 65 ps has been achieved by averaging 7 strips. Deeper analysis including photon loss by the gaps between strips has to be carried out.

Another possibility to increase the detector performance is to shrink the Cherenkov photon band by choosing a specific wavelength detection range in combination with other MCP-PMT types that have an enhanced QD in the red spectrum. This could be done by narrowing the QE range of the photon sensors or by optical filters with different wavelength cuts. Simplified MC simulations have shown promising first results. However, for the currently foreseen photo cathodes with a high QE in the blue spectrum, the photon yield at larger wavelengths is not sufficient to guarantee the desired performance goal.

A third alternative for increasing the resolution can be found in changing the mirror shape of the FELs. The geometrical aberration does only apply to non-paraxial photons. From the left side of figure 10, the following equation can be derived for the variation of the focal length with respect to the distance to the photon impact parametre h:

$$f(h) = R\left(1 - \frac{R}{2\sqrt{R^2 - h^2}}\right) \tag{5.1}$$

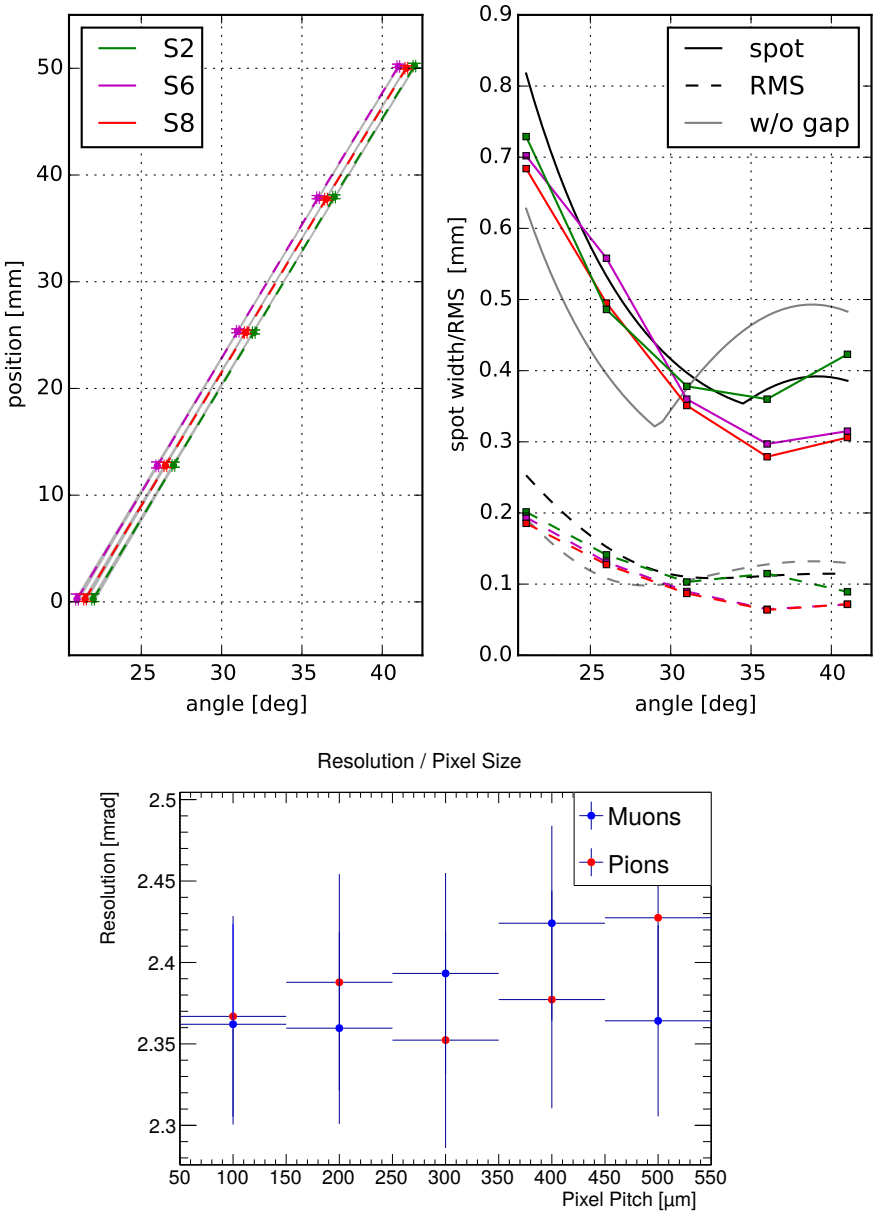

Figure 9. The measured focal spot width for different FEL samples (top) and the Cherenkov angle resolution for different pixel pitches (bottom). The focal spot measurements have been performed for 3 samples identified with S2, S6, and S8. The position information refers to the position on the MCP-PMT photocathode along one column, whereas the spot width indicates the photon position uncertainty due to the cylindrical mirror.

This formula can be expanded into a Taylor series with the following result:

$$f(h) \approx \frac{R}{2} - \frac{h^2}{4R} - \frac{3h^4}{16R^3} - \dots \tag{5.2}$$

Because the problem is fully symmetric, the terms with uneven exponents vanish completely. If all terms with exponents above 2 are neglected, the obtained result is already a sufficient approximation for small distances h and can be used for the design of a better asymmetric FEL. However, the

2020 JINST 15 C02032

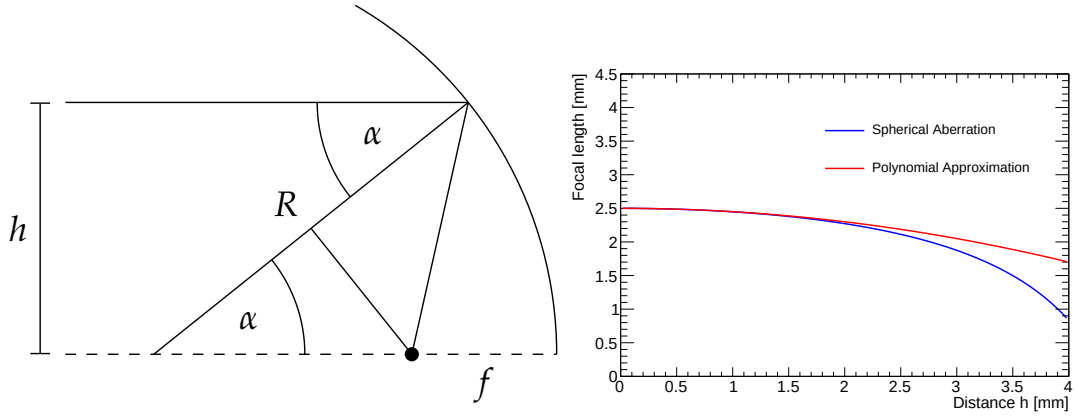

Figure 10. Geometrical aberration for a spherical mirror (left) and correction effects with aspherical mirror design (right).

fabrication of such an aspherical design is more complicated and costly. One of the major challenges will be to find a manufacturer who is able to provide the accurate polishing of a polynomial surface with a certain accuracy.

6 Conclusion & outlook

The simulation studies of possible DIRC options for the future SCTF detectors show promising results. Yet, several optimization steps are necessary in order to obtain the desired resolution of around 0.7 mrad that is required to separate muons and pions with a separation power of at least 3 s.d. at a momentum of 1.5 GeV/c. The two dominating effects are the angular straggling in the radiator material and the Cherenkov angle smearing as a result of dispersion. It is assumed, that an additional tracking detector with a resolution of a few hundred micrometers behind the Cherenkov counters could be used to reduce this effect for better detector performance. In combination with a new design of the FELs and the adaption of other sensor types, the desired performance goal is within reach. In addition to taking care of the required resolution, the high luminosity and resulting radiation damages have to be considered for choosing the right readout electronics. Currently, the required simulation studies are ongoing and further results will be published in the near future. To sum up, DIRC detectors are a promising alternative to other proposed PID systems in the SCTF detector and worthy to be considered as possible subdetectors.

References

[1] L. Shekhtman, F. Ignatov and V. Tayursky, *Simulation of physics background in Super c-tau factory detector*, *EPJ Web Conf.* **212** (2019) 01009.

[2] A.E. Bondar, *Project of a Super Charm-Tau factory at the Budker Institute of Nuclear Physics in Novosibirsk*, *Phys. Atom. Nucl.* **76** (2013) 1072.

[3] A.Yu. Barnyakov et al., *Particle identification system for the Super Charm-Tau Factory at Novosibirsk*, *Nucl. Instrum. Meth.* **A** (2019), in press.

[4] K. Föhl et al., *The Endcap Disc DIRC detector of PANDA*, *Nucl. Instrum. Meth.* **A 936** (2019) 588.

2020 JINST 15 C02032

[5] C. Schwarz et al., *The Barrel DIRC detector of PANDA*, *Nucl. Instrum. Meth.* **A 936** (2019) 586 [arXiv:1901.08432].

[6] K. Inami, *Development of Belle-II TOP detector and its MCP-PMT*, PoS(ICHEP2016)830.

[7] PANDA collaboration, *The Innovative Design of the Endcap Disc DIRC Detector for PANDA at FAIR*, in proceedings of the *Meeting of the Division of Particles and Fields of the American Physical Society (DPF2019)*, Boston, Massachusetts, 29 July–2 August 2019, arXiv:1909.09780.

[8] M. Schmidt et al., *Particle identification algorithms for the PANDA Endcap Disc DIRC*, 2017 *JINST* **12** C12051.

[9] C. Patrignani, *Review of Particle Physics*, *Chin. Phys.* **C40** (2016) 100001.

[10] O. Merle, *Development, design and optimization of a novel Endcap DIRC for PANDA*, PhD thesis, University of Giessen, Gießen (2014).

[11] K. Doroud and M. Williams, *A new approach for improved time and position measurements for TOF-PET: Time-stamping of the photo-electrons using analogue SiPMs*, *Nucl. Instrum. Meth.* **A 849** (2017) 16.

2020 JINST 15 C02032